UC Irvine

UC Irvine Previously Published Works

Title

Photon path distributions in turbid media: applications for imaging

Permalink

ISBN

Authors

Fantini, Sergio
Franceschini, Maria-Angela
Walker, Scott A
et al.

Publication Date

DOI

Copyright Information

Peer reviewed

Photon path distributions in turbid media: applications for imaging

Sergio Fantini, Maria Angela Franceschini, Scott A. Walker, John S. Maier, and Enrico Gratton

Laboratory for Fluorescence Dynamics,
Department of Physics, University of Illinois at Urbana-Champaign,
1110 West Green Street, Urbana, Illinois 61801-3080

ABSTRACT

Near-infrared optical tomography is thwarted by the highly scattering nature of light propagation in tissue. We propose a weighted back-projection method to produce a spatial map of an optical parameter which characterizes the investigated medium. We have studied the problem of the choice of the back-projection weight function for the absorption coefficient (μ_a) and for the reduced scattering coefficient (μ_s') of tissuelike phantoms. Working in frequency-domain optical imaging, we have initially approached the problem of quantifying the effect caused by a small absorbing defect embedded in the medium on the measured DC intensity, AC amplitude, and phase. The collection of DC, AC, and phase changes during a 1 mm step raster scan of the absorbing defect provides information on the photon path distributions and, in general, on the probed spatial region when DC, AC, and phase are, respectively, the measured parameters. We report experimentally determined weight functions for μ_a and μ_s'. They indicate that absorption and scattering maps can significantly differ in terms of resolution.

Keywords: Near-infrared optical tomography, back-projection, weight function, frequency-domain imaging, photon migration, photon paths, absorption coefficient, reduced scattering coefficient.

1. INTRODUCTION

Optical tomography in the near-infrared is an attractive tool for non-invasive, real time imaging of biological tissue. However, since most tissues act as strongly scattering media for near-infrared light, photons propagate diffusively from light source to optical detector. For this reason, instead of a single photon path, there is a distribution of photon paths inside the medium. This constitutes a complication of the imaging problem treated in the framework of x-ray Computerized Tomography (CT). A possible approach to tackle the inverse problem in optical tomography is to initially find a way to solve the forward problem. Then one can proceed iteratively to find the distribution of values of the optical properties inside the reconstruction region which is consistent with the results of the experimental measurement.[1-3] This approach, which is rigorous and formally correct, presents several difficulties in the critical choice of the computer algorithm, in the possibility of leading to non-unique solutions, and in the long time required to get the result. A simplified method for tomographic reconstruction is a weighted back-projection scheme, which has been applied in optical imaging by Barbour *et al.* to obtain intensity images of scattering media.[4,5] In order to obtain spatial maps of a physical property f of the investigated medium, we propose an alternative back-projection scheme in which the measured value of f from a particular source-detector configuration is assigned to a broad spatial region. Each point in this region is also assigned a weight, specified by an appropriate weight function. The tomographic image of

the measured physical parameter is finally built by superimposing, point by point, the weighted contributions from all source-detector configurations. This paper treats the problem of determining the weight function and relates such weight function to the photon path distributions in the medium.

2. BACK-PROJECTION OPERATOR

2.1 X-ray tomography

In x-ray tomography, where the paths of the probing particles (x-photons) from source to detector can be assumed to be straight lines, it is possible to define a back-projection operator in terms of one-dimensional integrals. Figure 1 defines the rectangular (x,y) and the polar (r,ϕ) coordinates used in modeling the imaging problem. L is the straight line joining source and detector, K is the line through the origin (O) and perpendicular to L, and P is the intersection point between L and K. Let $f(r,\phi)$ be a physical parameter which is function of the position in the reconstruction region (Ω), and let us assume $f(r,\phi) = 0$ for $(r,\phi) \notin \Omega$. A projection operator, which projects all the values of $f(r,\phi)$ in L on the line K, can be defined in terms of the Radon transform $\Re$ (Ref. [6]):

$$[\Re f](\ell,\alpha) = \int_{-\infty}^{+\infty} f\left(\sqrt{\ell^2 + z^2}, \alpha + \tan^{-1}(z / \ell)\right) dz \tag{1}$$

where (ℓ,α) defines the line L ($\ell = \overline{OP}$ and $\alpha = P\hat{O}X$), and the integral is a line integral of $f(r,\phi)$ along L.
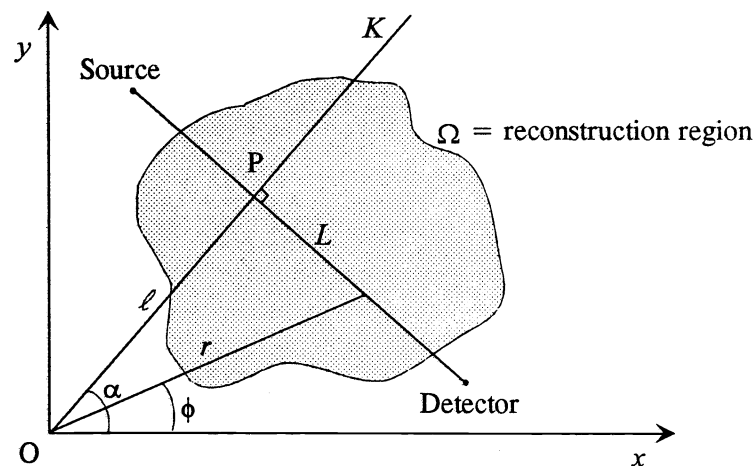

Fig. 1. Geometry of the problem of tomographic reconstruction of the space region Ω. (x,y) are the rectangular coordinates, whereas (r,ϕ) are the polar coordinates. L is the straight line joining source and detector. K is the line through the origin (O) orthogonal to L in P. The coordinates $\ell = \overline{OP}$ and $\alpha = P\hat{O}X$ define the line L and hence the source-detector configuration.

In x-ray tomography, the contributions to the measured quantity from all the points in $L \cap \Omega$ are assumed to be the same and sum up linearly. Hence, $[\Re f](\ell,\alpha)$ is proportional to the measured value of

the physical parameter f in the source-detector geometrical configuration (ℓ,α). One can define a back-projection operator $\aleph$ to assign a value of $f(r,\phi)$ to all the points in Ω, on the basis of the experimental results relative to all possible lines L which intersect Ω. The idea is to back project the measured value $[\Re f](\ell,\alpha)$ over all the points in Ω along L and sum the contributions from all source-detector pairs. The assigned value of f to the point (r,ϕ) can be written $[\aleph[\Re f](\ell,\alpha)](r,\phi)$ and defined as:[6]

$$\left[\aleph[\Re f](\ell,\alpha)\right](r,\phi) = \int_0^\pi [\Re f]\left(r\cos(\alpha-\phi),\alpha\right)d\alpha \tag{2}$$

In Eq. (2) the integral sums up the contributions from all the lines L passing through (r,ϕ).

2.2 Near-infrared tomography

In near-infrared optical tomography, the photon paths in tissue are distributed over a 3-D region, which is sometimes called a *light bundle*, so that the line integral in Eq. (1) is replaced by a volume integral. Furthermore, the photon path density is not uniformly distributed over the light bundle, and for this reason a position dependent weight function $W_f^{(\alpha)}(\mathbf{r})$ must be introduced. In optical imaging, a normalized operator $(\Im)$ which generalizes Eq. (1) can thereby be defined as a weighted average of the values of $f(\mathbf{r})$ over the volume of the light bundle (i.e. over the domain of $W_f^{(\alpha)}(\mathbf{r})$):

$$[\Im f](\alpha) = \frac{\int W_f^{(\alpha)}(\mathbf{r})f(\mathbf{r})d^3\mathbf{r}}{\int W_f^{(\alpha)}(\mathbf{r})d^3\mathbf{r}} \tag{3}$$

where α is the six-component vector which defines the source-detector geometrical configuration (by defining the positions of source and detector). Similar to the x-ray case, a back-projection operator can be defined. For a discrete number N of source-detector configurations α_i, it can be written as follows:

$$[\aleph[\Im f](\alpha)](\mathbf{r}) = \frac{\sum_{i=1}^{N}[\Im f](\alpha_i)W_f^{(\alpha_i)}(\mathbf{r})}{\sum_{i=1}^{N}W_f^{(\alpha_i)}(\mathbf{r})} \tag{4}$$

The approach to the problem of imaging presented in this Section requires that the contributions to the measured value of f from each voxel is independent of that from all the other voxels. In optical tomography this is not true, but as long as small perturbations are considered, it constitutes a reasonable approximation.

3. PHOTON PATH DISTRIBUTIONS IN TURBID MEDIA

3.1 Continuous wave (CW) light

Light propagation in turbid media is modeled by the diffusion approximation to the Boltzmann transport equation. Analytical solutions for the photon flux distribution in macroscopically homogeneous media and for several boundary conditions have been determined.[7] The presence of macroscopic inhomogeneities which have small influence on the measured quantities have been treated within the framework of perturbation theory.[8,9] In the case that the inhomogeneity is a small (linear dimensions much less than source-detector distance) totally absorbing defect, one can assume that the decrease in intensity (defined as $1-I_{DC}(\mathbf{r})/I_{DC0}$ where $I_{DC}(\mathbf{r})$ is the detected intensity when the defect is in $\mathbf{r}$ and I_{DC0} is the detected intensity in the absence of the defect) caused by this defect is proportional to the photon path density at the position of the defect. In this way, the photon path distributions in turbid media have been studied both experimentally[10] and theoretically.[8] In this perspective, the probability $p_{DC}(\mathbf{r},\mathbf{r}_s,\mathbf{r}_d)$ that a photon emitted at $\mathbf{r} = \mathbf{r}_s$ (source position) *and* detected at $\mathbf{r} = \mathbf{r}_d$ (detector position) passes through $\mathbf{r}$ is analytically given, in the infinite geometry and for CW light, by Ref. [9] as:

$$p_{DC}(\mathbf{r},\mathbf{r}_s,\mathbf{r}_d) = 1 - \varepsilon_{DC}(\mathbf{r},\mathbf{r}_s,\mathbf{r}_d) = 1 - \frac{\dfrac{\exp\left(-\sqrt{\dfrac{\mu_a}{D}}|\mathbf{r}_d - \mathbf{r}_s|\right)}{|\mathbf{r}_d - \mathbf{r}_s|} - \dfrac{\Delta\mu_a\Delta V}{4\pi D}\dfrac{\exp\left(-\sqrt{\dfrac{\mu_a}{D}}\left(|\mathbf{r} - \mathbf{r}_s| + |\mathbf{r}_d - \mathbf{r}|\right)\right)}{|\mathbf{r} - \mathbf{r}_s||\mathbf{r}_d - \mathbf{r}|}}{\dfrac{\exp\left(-\sqrt{\dfrac{\mu_a}{D}}|\mathbf{r}_d - \mathbf{r}_s|\right)}{|\mathbf{r}_d - \mathbf{r}_s|}} \tag{5}$$

where $\varepsilon_{DC}(\mathbf{r},\mathbf{r}_s,\mathbf{r}_d)$ is defined as $I_{DC}(\mathbf{r})/I_{DC0}$, μ_a is the absorption coefficient of the medium, D is the diffusion coefficient defined as $1/(3\mu_a+3\mu_s')$ with μ_s' reduced scattering coefficient, $\Delta\mu_a$ is the difference between the absorption coefficient of the defect and that of the background, and ΔV is the volume occupied by the defect. The probability $p_{DC}(\mathbf{r},\mathbf{r}_s,\mathbf{r}_d)$ does not directly define the light bundle. We can define the light bundle by giving its sectional surface $S_{\tilde{x}}$ at every point $\tilde{x}$ of the line joining source and detector, which we will call the x-axis. In the infinite geometry, we define $S_{\tilde{x}}$ as the circle in the plane $x = \tilde{x}$ and with the center in the x-axis which obeys:

$$\frac{\displaystyle\iint_{S_{\tilde{x}}} p_{DC}(\tilde{x},y,z,\mathbf{r}_s,\mathbf{r}_d)\,dydz}{\displaystyle\int_{-\infty}^{+\infty}\int_{-\infty}^{+\infty} p_{DC}(\tilde{x},y,z,\mathbf{r}_s,\mathbf{r}_d)\,dydz} = 0.8 \tag{6}$$

where the value 0.8 is arbitrarily chosen and corresponds to the selection of 80% of the photon paths through $x = \tilde{x}$.

3.2 Intensity modulated light

In frequency-domain imaging, the intensity of the light source is modulated at a frequency of the order of 100 MHz, and, besides average intensity (DC), there are two additional measurable parameters: the amplitude of the intensity oscillations (AC) and the phase (Φ) of the intensity wave at the modulation frequency. The effect of a totally absorbing defect on the measured value of AC is in general different than that on the measured DC. The difference is a function of the modulation frequency. It is possible to express the variations in measured AC and phase (ε_{AC} and ε_{Φ} respectively) due to the presence of a totally absorbing point-like defect in $\mathbf{r}$. $\varepsilon_{AC}(\mathbf{r},\mathbf{r}_s,\mathbf{r}_d)$ is defined as $I_{AC}(\mathbf{r})/I_{AC0}$, while $\varepsilon_{\Phi}(\mathbf{r},\mathbf{r}_s,\mathbf{r}_d)$ is defined as the difference $\Phi(\mathbf{r})-\Phi_0$ with $\Phi(\mathbf{r})$ phase measured with the defect in $\mathbf{r}$ and Φ_0 phase measured in the absence of the defect. By following the approach presented in Ref. [9] we have:

$$\varepsilon_{AC}(\mathbf{r},\mathbf{r}_s,\mathbf{r}_d) = \text{Abs}\left(\frac{I_{AC}(\mathbf{r})}{I_{AC0}}\right) \tag{7}$$

$$\varepsilon_{\Phi}(\mathbf{r},\mathbf{r}_s,\mathbf{r}_d) = \text{Arg}\left(\frac{I_{AC}(\mathbf{r})}{I_{AC0}}\right) \tag{8}$$

with:

$$\frac{I_{AC}(\mathbf{r})}{I_{AC0}} = 1 - \frac{\Delta\mu_a \Delta V}{4\pi D} \frac{\dfrac{\exp\left(-\sqrt{\dfrac{\mu_a}{2D}}\left(\sqrt{1+x^2}+1\right)^{1/2}\left(|\mathbf{r}-\mathbf{r}_s|+|\mathbf{r}_d-\mathbf{r}|\right)+i\sqrt{\dfrac{\mu_a}{2D}}\left(\sqrt{1+x^2}-1\right)^{1/2}\left(|\mathbf{r}-\mathbf{r}_s|+|\mathbf{r}_d-\mathbf{r}|\right)\right)}{|\mathbf{r}-\mathbf{r}_s||\mathbf{r}_d-\mathbf{r}|}}{\dfrac{\exp\left(-\sqrt{\dfrac{\mu_a}{2D}}\left(\sqrt{1+x^2}+1\right)^{1/2}|\mathbf{r}_d-\mathbf{r}_s|+i\sqrt{\dfrac{\mu_a}{2D}}\left(\sqrt{1+x^2}-1\right)^{1/2}|\mathbf{r}_d-\mathbf{r}_s|\right)}{|\mathbf{r}_d-\mathbf{r}_s|}}$$

where x is defined as $\omega/(\nu\mu_a)$ with ω angular modulation frequency and ν velocity of light in the medium.

We note the different physical meaning of the three quantities $\varepsilon_{DC}(\mathbf{r},\mathbf{r}_s,\mathbf{r}_d)$, $\varepsilon_{AC}(\mathbf{r},\mathbf{r}_s,\mathbf{r}_d)$ and $\varepsilon_{\Phi}(\mathbf{r},\mathbf{r}_s,\mathbf{r}_d)$.
$\varepsilon_{DC}(\mathbf{r},\mathbf{r}_s,\mathbf{r}_d)$, as already discussed, is related to the photon path distribution in the medium in CW conditions;
$\varepsilon_{AC}(\mathbf{r},\mathbf{r}_s,\mathbf{r}_d)$ has a similar interpretation, but it refers to the AC signal detected in the frequency-domain. The physical reason for the difference between $\varepsilon_{DC}(\mathbf{r},\mathbf{r}_s,\mathbf{r}_d)$ and $\varepsilon_{AC}(\mathbf{r},\mathbf{r}_s,\mathbf{r}_d)$ is that the attenuation of the DC (or CW) component of light intensity is smaller than that of the AC component of light intensity;
$\varepsilon_{\Phi}(\mathbf{r},\mathbf{r}_s,\mathbf{r}_d)$ gives information on the spatial region effectively probed when the phase Φ is the measured parameter. Larger values of $\varepsilon_{\Phi}(\mathbf{r},\mathbf{r}_s,\mathbf{r}_d)$ mean a larger effect on the measured phase due to the deletion of photon paths through $\mathbf{r}$.
In Fig. 2, panels (a), (b), (c) we present gray scale plots of the theoretical expressions for ε_{DC}, ε_{AC}, and ε_{Φ} respectively. Eqs. (5), (7), and (8) are evaluated for the following values of the parameters:
$\Delta\mu_a$=3 cm^{-1}, ΔV=0.014 cm^3, ω = $2\pi\times$120 MHz, μ_a = 0.03 cm^{-1}, μ_s' = 19 cm^{-1}.
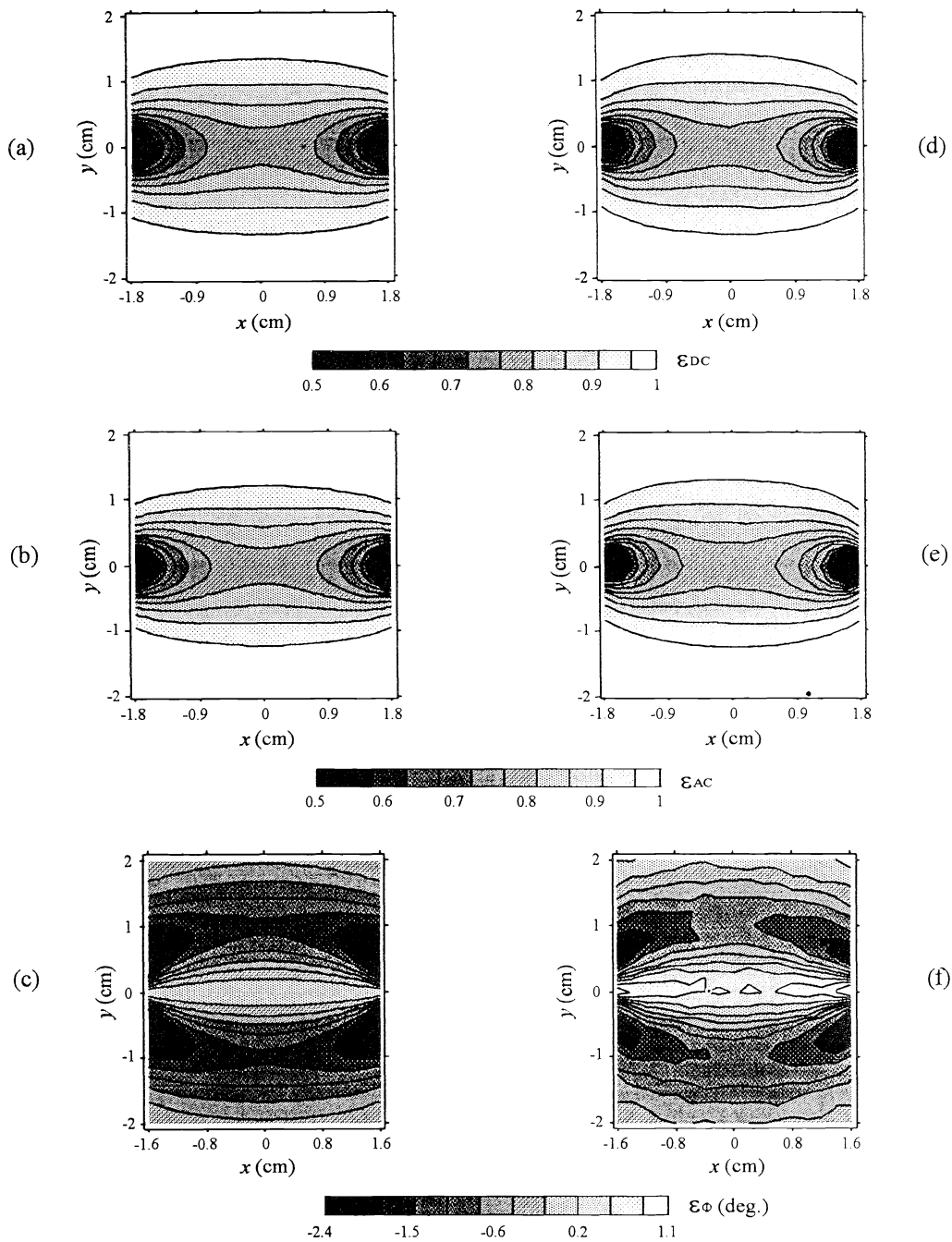
Fig. 2. Effect of a small totally absorbing defect (3 mm in diameter) scanned in the x-y plane on the measured DC (panels (a) and (d)), AC (panels (b) and (e)), and phase (panels (c) and (f)) at 120 MHz modulation frequency. Source and detector (not shown) are located respectively in (-2,0) and (2,0), and are deeply immersed in a strongly scattering medium (μ_a=0.03 cm^{-1}, μ_s'=19 cm^{-1}). The gray level at each point (x,y) corresponds to the value of the plotted quantity relative to the case in which the defect is located in that point (x,y). The left panels are theoretical predictions for ε_{DC} (panel (a)), ε_{AC} (panel (b)), and ε_{Φ} (panel (c)). The right panels are experimental results for ε_{DC} (panel (d)), ε_{AC} (panel (e)), and ε_{Φ} (panel (f)). The gray levels are quantified by the palettes underneath each pair of figures.

To experimentally verify these equations, we have conducted an experiment in which both the light source (laser diode emitting light at 780 nm) and the detector fiber (3 mm in diameter) were deeply immersed in an aqueous Liposyn solution (infinite geometry). A small black sphere (3 mm in diameter corresponding to $\Delta V = 0.014$ cm^3) was scanned at 1 mm steps on the plane containing source and detector. The modulation frequency was 120 MHz, and the values of μ_a and μ_s' of the Liposyn solution were 0.03 cm^{-1} and 19 cm^{-1} respectively (matching the values used to calculate $\varepsilon_{DC}(r,r_s,r_d)$, $\varepsilon_{AC}(r,r_s,r_d)$ and $\varepsilon_{\Phi}(r,r_s,r_d)$ plotted in Fig. 2 (a), (b), and (c)). In Fig. 2 (d), (e), and (f) we plot the measured variations in DC, AC, and phase (respectively) recorded during the scan of the sphere. The value of $\Delta\mu_a = 3$ cm^{-1} (employed to evaluate the theoretical predictions) was chosen to recover the experimental value of $I(0,0)/I_0 = 0.19$. The comparison between theoretical predictions and experimental results shows an excellent agreement and confirms the validity of the perturbation approach to treat the problem of small defects.

4. DETERMINATION OF THE WEIGHT FUNCTION $W_f^{(\alpha)}(r)$

The DC, AC, and phase defect-induced variations discussed in the last Section give information on the sensitivity of each directly measured quantity to the deletion of photon paths through a specific point of space. If $f(r)$ is a physical parameter of the medium and f_m is its measured value with a particular source-detector pair α as a function of DC, AC, and phase, we can write $f_m^{(\alpha)} = F^{(\alpha)}(DC, AC, \Phi)$. We define the weight function for $f(r)$ as:

$$W_f^{(\alpha)}(r) = \left| \frac{F^{(\alpha)}(DC, AC, \Phi)\Big|_{\text{defect in } r} - F_0^{(\alpha)}(DC, AC, \Phi)}{F_0^{(\alpha)}(DC, AC, \Phi)} \right| \tag{9}$$

where F_0 is the measured value of f in the absence of the defect. By taking into account the fact that we are considering small perturbations we can also write the weight function in terms of the changes in DC, AC, and phase as:

$$W_f^{(\alpha)}(r) \approx \left| \frac{\dfrac{\partial F^{(\alpha)}}{\partial(DC)}\bigg|_{DC_0} \varepsilon_{DC} + \dfrac{\partial F^{(\alpha)}}{\partial(AC)}\bigg|_{AC_0} \varepsilon_{DC} + \dfrac{\partial F^{(\alpha)}}{\partial\Phi}\bigg|_{\Phi_0} \varepsilon_{\Phi}}{F_0^{(\alpha)}} \right| \tag{10}$$

where DC_0, AC_0, and Φ_0 are the measured DC, AC, and Φ in the absence of the defect.

We have applied Eq. (9) to the results of the experiment in which we scanned the small absorbing defect in the plane containing source and detector. For each position of the defect we calculated μ_a and μ_s' with the pre-calibrated measurement protocol described elsewhere.[11] The results for the weight functions for μ_a and μ_s', which quantify the effect of the deletion of photon paths through a specific point of space on the recovered values of μ_a and μ_s', are plotted in Fig. 3. It is noteworthy the difference

between the two weight functions for μ_a and μ_s'. That is due to the different functional dependence of μ_a and μ_s' on the directly measured parameters DC and phase.
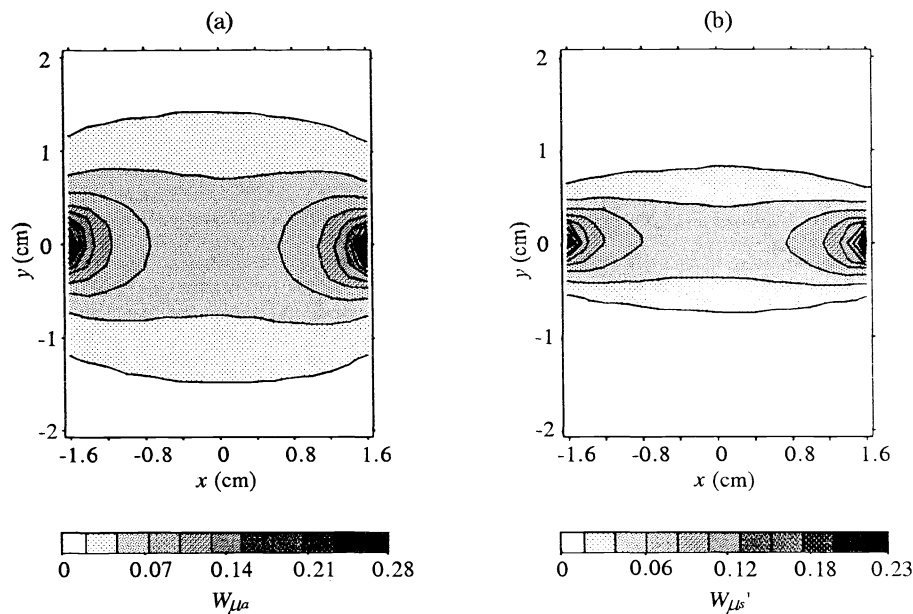

Fig. 3. Experimentally determined weight functions for absorption coefficient (panel (a)) and reduced scattering coefficient (panel (b)). The gray levels are quantified by the palettes, and the meaning of x and y axes, as well as the positions of source and detector, are the same as in Fig. 2.

5. DISCUSSION AND CONCLUSION

We stress that Fig. 2 does not provide a representation of the light bundle, which is rigorously defined by Eq. (bundle) in terms of $p_{DC}(\mathbf{r},\mathbf{r_s},\mathbf{r_d})$. This light bundle, which contains the majority of the photon paths from source to detector, specifies the geometrical properties of diffusive light propagation from source to detector. We are currently exploring the connection among these geometrical properties, the wavelength of the photon-density wave, and the resolution attainable in optical imaging. In the case in which DC, AC, and phase are combined to yield a physical quantity, the weight function for that quantity provides resolution information. In this perspective, Fig. 3 suggests that, at least in our experimental conditions, a scattering image should be better resolved than an absorption image. In fact, this is what we found in a series of experiments on phantoms containing scattering and absorbing inhomogeneities.[11]

A problem in the determination of the weight function for the quantity f is that the weight function depends on the value of f of the background medium. This difficulty could be overcome by performing a measurement of the average value of f over the reconstruction region and by calculating the weight function using that average value. We are currently evaluating the sensitivity of W_{μ_a} and $W_{\mu_s'}$ on changes in the optical properties of the background medium.

The back-projection method presented in this paper constitutes a simplification of the mathematically rigorous reconstruction algorithm based on the inversion of the integral operator $\Im$

defined in Eq. (3). The major advantage of the back-projection method is that it is fast, in terms of computation time, and always yields a unique solution. For this reason, in addition to fast acquisition times for optical data, can be used to provide real time optical tomography, which would constitute a considerable step forward with respect to current tomographic techniques. We estimate that an optical image of a region with linear dimensions of about 5 cm could be updated every few seconds. On the other hand, the back-projection method is likely to produce blurred images. The reason for this is that we assign a single reading value, which could be mainly due to a localized inhomogeneity, to a broad spatial region. An appropriate weight function will partially correct for this problem, but it still remains as a characteristic feature of back-projection. Also, a highly resolved and contrasted image requires a high number N of source detector configurations, i.e. the summation in Eq. (4) should contain many significant ($W_f^{(\alpha_i)} \neq 0$) terms.

In conclusion, we have described a weighted back-projection scheme designed to yield a spatial map of a physical property of the investigated medium. Working in frequency-domain imaging, we have studied the effect of the deletion of the photon paths through a specific point of space on the measured DC, AC, and phase. In particular, we have related the effect on the DC intensity to the photon path distributions between light source and optical detector. Finally, we have defined and experimentally derived the weight functions for absorption ($W_{\mu_a}(\mathbf{r})$) and for reduced scattering coefficient ($W_{\mu_s'}(\mathbf{r})$). They should be interpreted as the relative change in the measured values of μ_a and μ_s', respectively, caused by the deletion of the photon paths through $\mathbf{r}$. The shape of these weight functions resembles that of $\varepsilon_{DC}(\mathbf{r})$ (i.e. $I_{DC}(\mathbf{r})/I_{DC0}$) but their width is determined by the particular functional dependence on the phase.

6. ACKNOWLEDGMENTS

7. REFERENCES

1. J. R. Singer, F. A. Grünbaum, P. Kohn, and J. Passamani Zubelli, "Image Reconstruction of the Interior of Bodies That Diffuse Radiation," Science **248**, 990-993 (1990).

2. S. R. Arridge, P. van der Zee, M. Cope, and D. T. Delpy, "Reconstruction Methods for Infra-Red Absorption Imaging," Proc. SPIE **1431**, 204-215 (1991).

3. B. W. Pogue and M. S. Patterson, "Forward and Inverse Calculation for Near-Infrared Imaging Using a Multigrid Finite Difference Method," Proc. *Advances in Optical Imaging and Photon Migration Topical Meeting*, Orlando, Florida (1994), *in press*.

4. R. L. Barbour, H. L. Graber, R. Aronson, and J. Lubowsky, "Imaging of Subsurface Regions of Random Media by Remote Sensing," Proc. SPIE **1431**, 192-203 (1991).

5. H. L. Graber, J. Chang, R. Aronson, and R. L. Barbour, "A Perturbation Model for Imaging in Dense Scattering Media: Derivation and Evaluation of Imaging Operators," in *Medical Optical Tomography: Functional Imaging and Monitoring*, G. J. Müller *et al.*, eds., **IS11**, 65-86 (1993).

6. G. T. Herman, *Image Reconstruction from Projections* (Academic, New York, 1980).

7. S. R. Arridge, M. Cope, and D. T. Delpy, "The Theoretical Basis for the Determination of Optical Pathlengths in Tissue: Temporal and Frequency Analysis," Phys. Med. Biol. **37**, 1531-1560 (1992).

8. S. F. Feng, F. Zeng, and B. Chance, "Monte Carlo Simulations of Photon Migration Path Distributions in Multiple Scattering Media," Proc. SPIE **1888**, 78-89 (1993).

9. J.-M. Kaltenbach and M. Kaschke, "Frequency- and Time-Domain Modelling of Light Transport in Random Media," in *Medical Optical Tomography: Functional Imaging and Monitoring*, G. J. Müller *et al.*, eds., **IS11**, 65-86 (1993).

10. W. Cui, C. Kumar, and B. Chance, "Experimental Study of Migration Depth for the Photons Measured at Sample Surface," Proc. SPIE **1431**, 180-191 (1991).

11. M. A. Franceschini, S. Fantini, S. A. Walker, J. S. Maier, and E. Gratton, "Multi-Channel Optical Instrument for Near-Infrared Imaging of Tissue," in *Optical Tomography, Photon Migration, and Spectroscopy of Tissue and Model Media: Theory, Human Studies, and Instrumentation*, Proc. SPIE **2389** (1995).